Sustinere
Journal of Environment and Sustainability
Volume 9 Number 1 (2025) 1-9

Print ISSN: 2549-1245 Online ISSN: 2549-1253
Website: https://sustinerejes.com E-mail: sustinere.jes@uinsaid.ac.id

RESEARCH PAPER

Effect of ammonium/phosphate molar ratio on struvite production via electrolysis using a sacrificial magnesium anode

Aditya Kurnia Aji Pangestu[1*], Arseto Yekti Bagastyo[1*], Ervin Nurhayati[1], Jr-Lin Lin[2], Fahrudin Sidik[2]
[1]*Dept. of Environmental Engineering, Faculty of Civil, Planning, and Geo-Engineering, Institut Teknologi Sepuluh Nopember, Surabaya 60111, Indonesia*
[2]*Dept. of Environmental Engineering, Chung Yuan Christian University, Chung-Li, Taiwan, ROC*

Article history:
Received 19 December 2024 | Accepted 9 January 2025 | Available online 30 April 2025

Abstract. Excessive ammonium and phosphate levels in aquatic environments potentially cause eutrophication, leading to water quality imbalance, algal blooming, and disturbance of biodiversity status. Electrolysis using a sacrificial magnesium anode effectively removes and recovers ammonium and phosphate, producing struvite ($MgNH_4PO_4.6H_2O$). The present study investigated the optimum current density and the effect of the ammonium/phosphate molar ratio on struvite production. The current density was controlled at 10, 50, and 100 mA/cm^2. An artificial wastewater containing [NH_4^+]:[PO_4^{3-}] in a molar ratio of 1:10, 1:1, and 10:1 was used as the test solution. The optimum current density was determined as 50 mA/cm^2. The ammonium and phosphate reduction ratios at a 1:1 molar ratio was approximately 46.91% and 74.26%, respectively. Increasing the ammonium molarity in the test solution to 10:1 increased the phosphate reduction ratio to 96.38% while decreasing the ammonium reduction ratio to 26.28%. The maximum precipitation of 4.1914 g was generated at a molar ratio of 10:1 with a specific energy consumption of 0.011 Wh/mg-P, out of the three ammonium/phosphate molar ratio variations. Microscopes and SEM-EDS were used to characterize the precipitates produced, and Visual MINTEQ 3.1 was then used for modeling.

Keywords: Ammonium and phosphate recovery; Electrolysis; Sacrificial magnesium anode; Struvite

1. Introduction

The ammonium and phosphate concentrations in wastewater, such as dairy and poultry wastewater approximately in a range of 1710-3400 mg NH_4^+/L and 1000-1800 mg PO_4^{3-}/L, respectively (Silva-Gálvez et al., 2024; Vaishnav et al., 2023; Ye et al., 2018). Once high ammonium and phosphate concentrations are found in aquatic environments via runoff, this condition further impacts eutrophication, leading to an imbalance in water quality, algae blooming, and disturbing the biodiversity status (Lin et al., 2023; Lin & Sidik, 2024; Ye et al., 2018). On the other hand, if ammonium and phosphate can be recovered, the availability of valuable resources that will decrease as supply-demand increases due to the life of these organisms can be controlled. Struvite

---

[*] Corresponding author. E-mail: aditya.kurnia.ap@gmail.com, bagastyo@enviro.its.ac.id

DOI: https://doi.org/10.22515/sustinere.jes.v9i1.473

($MgNH_4PO_4.6H_2O$, MAP) is a slow-release fertilizer with a white orthorhombic crystalline structure formed from a combination of magnesium, ammonium, and phosphate (Bagastyo et al., 2022; Kim et al., 2007). Struvite is influenced by the pH, supersaturation, and ion molar ratio (Wang et al., 2022).

Several studies have reported that struvite formation can be removed by more than 80% using a stirred tank reactor (STR) (Siciliano et al., 2020). The selection of the Mg source is a critical consideration in struvite production because it significantly affects both the quality and production cost. Commonly used magnesium sources include $MgCl_2$, $MgSO_4$, $Mg(OH)_2$, MgO, magnesite, and magnesium alloys, with their respective advantages and disadvantages. On average, magnesium sources from chemicals are expensive and produce byproducts (Bagastyo et al., 2022). Because of the lack of other sources, magnesium alloy is a potential source of Mg for struvite formation as a sacrificial anode.

Initial study on electrolysis using a magnesium sacrificial anode. Their study achieved a phosphate removal rate of 59-84% at an initial pH of 8.9 (Hug & Udert, 2013). In another study, the recovery rates were 5.24 mg-P/h.cm^2 in synthetic digestion fluids and 4.60 mg-P/h.cm^2 in anaerobically digested chicken manure slurry (Luo et al., 2022). Based on these results, the use of a magnesium alloy as a sacrificial anode in electrolysis has the potential to recover ammonium and phosphate by struvite production.

The study investigated the effect of current density on magnesium-plate corrosion and the effect of ammonium/phosphate molar ratio on struvite production. Specific objectives were to determine the effect of the ammonium/phosphate molar ratio on struvite production. The energy consumption of the process was also calculated to ensure that the process was energy-efficient.

2. Materials and methods

2.1 Materials

To obtain the optimum current density in terms of magnesium alloy released under electrochemical operation, 3.5% sodium chloride (NaCl, Sigma-Aldrich) was used as a background solution. On the other hand, 500 mL of artificial wastewater containing ammonium and phosphate corresponding to ammonium/phosphate molar ratios of 1:10 (0.0016 mol-N/L:0.0161 mol-P/L), 1:1 (0.0161 mol-N/L:0.0161 mol-P/L), and 10:1 (0.1614 mol-N/L:0.0161-P/L) were used as the test solution. The sources of ammonium and phosphate were taken from ammonium chloride (NH_4Cl, Honeywell) and potassium phosphate dibasic (K_2HPO_4, Sigma-Aldrich), respectively. An AZ31B (Al 3 wt%, Zn 1 wt%, balance Mg) magnesium alloy was used as a sacrificial anode in the electrolysis process to release Mg^{2+} ions into the solution. The anode dimension was 49 x 100 mm with a thickness of 2 mm (active surface area was 14.7 cm^2). A 316SS stainless steel was used as the cathode in the electrolysis process. The cathode dimension was 49 x 100 mm with a thickness of 1.8 mm (active surface area was 14.7 cm^2).

2.2 Experimental setup

The study was conducted at a laboratory scale using 0.6-L-beaker glass modified with the addition of an electrode hanger as the main reactor. The current was applied by a DC power supply (Gophert CPS3205, China) with current density variations of 10, 50, and 100 mA/cm^2. The pH was controlled at 9±0.5 by the addition of 1 M HCl or 1 M NaOH during the process and continuously stirred at approximately 150 rpm for 30 min in batch recirculation mode. The solution was passed through a peristaltic pump from the main reactor to the monitoring tank and vice versa. The pH and conductivity (HACH HQ430d, USA) sensors were placed in a 100 mL beaker, which served as the monitoring tank. An AZ31B Mg alloy was employed as the anode, whereas a 316SS stainless steel was employed as the cathode, with the distance between the electrodes held at 2 cm. A schematic of the electrolysis experiment setup is shown in Figure 1.

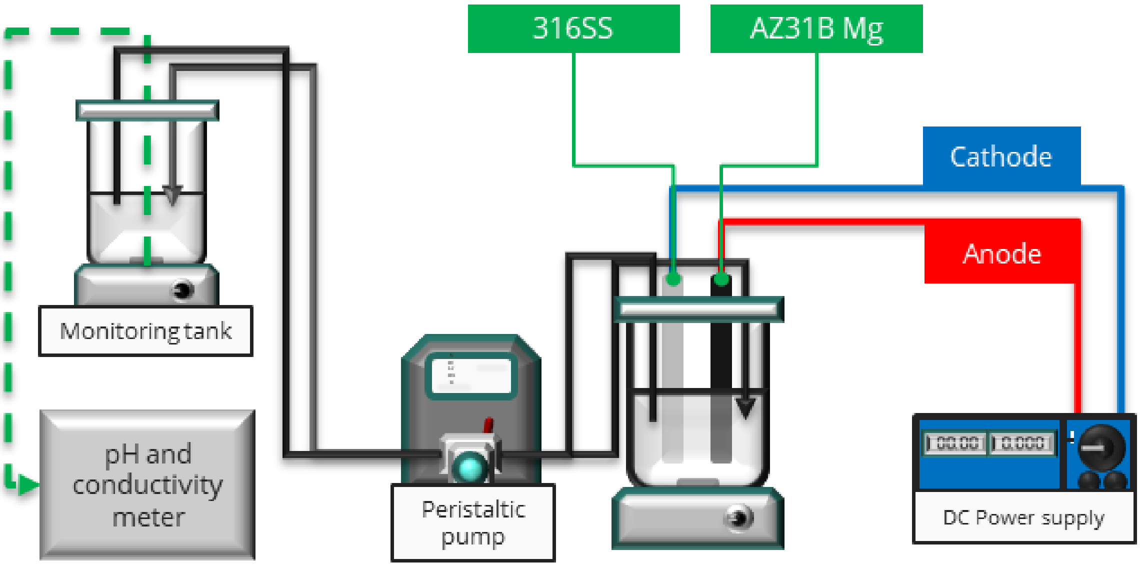

Figure 1. Schematic of the electrolysis experiment

2.3 Analytical methods

The actual/calculation ratio of AZ31B Mg alloy released ion in terms of mass was investigated to determine the optimum current density. The expected Mg mass was calculated using the Faraday equation (Equation 1).

$$m_{Mg} = \frac{M_{Mg} \times I \times t}{z \times F} \tag{1}$$

where m_{Mg} (g) is the expected magnesium release, M_{Mg} is the Mg molar mass (24.3 g/mol), I (A) is the applied current, z is the magnesium valence (2), and F is the Faraday constant (96485 C/mol) (Kékedy-Nagy et al., 2020).

The precipitate formed from the test solution was collected and recovered by vacuum filtration (Rocker 300, Taiwan), where the filter holder was fitted with a PTFE un-laminated polytetrafluoroethylene membrane filter (0.45-µm, 47 mm). The mass of electrochemically precipitated struvite was determined using an analytical balance (XS225A, Switzerland). The visual and morphological analysis of struvite was investigated using microscopes and SEM-EDS, respectively. The EDS data were analyzed by a modeling method using Visual MINTEQ 3.1. Ammonium and phosphate concentrations were measured using a UV spectrophotometer (Spectramax ABS, US) using the indophenol and ascorbic acid method, whereas magnesium ion was measured by ICP measurement.

3. Result and discussion

3.1. Effect of current density on releasing Mg^{2+} ions

The current density was shown to affect the release of mg ions after 30 min of the experiment. At a current density of 10 mA/cm^2, the weight of the magnesium plate was reduced by 0.0126 grams. Furthermore, the background solution contained 0.80 mol/L of dissolved magnesium resulting from the decay of magnesium plates. At current densities of 50 and 100 mA/cm^2 also experienced the same thing where magnesium plates reduced by 0.1198 and 0.4593 g, respectively. At this current density, magnesium was found in background solutions of 1.90 and 1.98 mol/L, respectively (Figure 2a). This condition is in accordance with research that showed that increasing the current density significantly enhances the release of magnesium ions from the magnesium anode during electrolysis. Higher current densities lead to increased energy consumption and can also affect the passivation of the anode, which is relevant to understanding how current density influences ion release dynamics (Cai et al., 2022).

When compared with the calculation using the Faraday equation (Equation 1) based on the reduction of the weight of the magnesium plate, it was known that the actual/theoretical calculation ratio closest to 1 was a current density of 50 mA/cm², with a difference of 0.2809, followed by a current density of 100 mA/cm², with a difference of 0.3784, and 10 mA/cm², with a difference of 0.6218 (Figure 2b). Differences between the theory based on the Faraday Equation and actual conditions also occurred in other studies, that dissolved mg ions under real conditions were much lower than the calculated values (Natsi & Koutsoukos, 2024). Thus, the optimum current density was 50 mA/cm² then be used in the study of the effect of the N/P molar ratio on struvite production.

3.2. Ammonium and phosphate reduction during the electrolysis

The concentrations of ammonium and phosphate in the test solution decreased positively for all N/P molar ratios at different levels (Figure 3). This indicates that both ammonium and phosphate react and bind to each other with the Mg ions released by the plates. This condition supports previous research reporting that the concentrations of ammonium and phosphate simultaneously decrease during the electrolysis process. This indicates that magnesium ions are crucial for the binding of ammonium and phosphate (Wang et al., 2022).

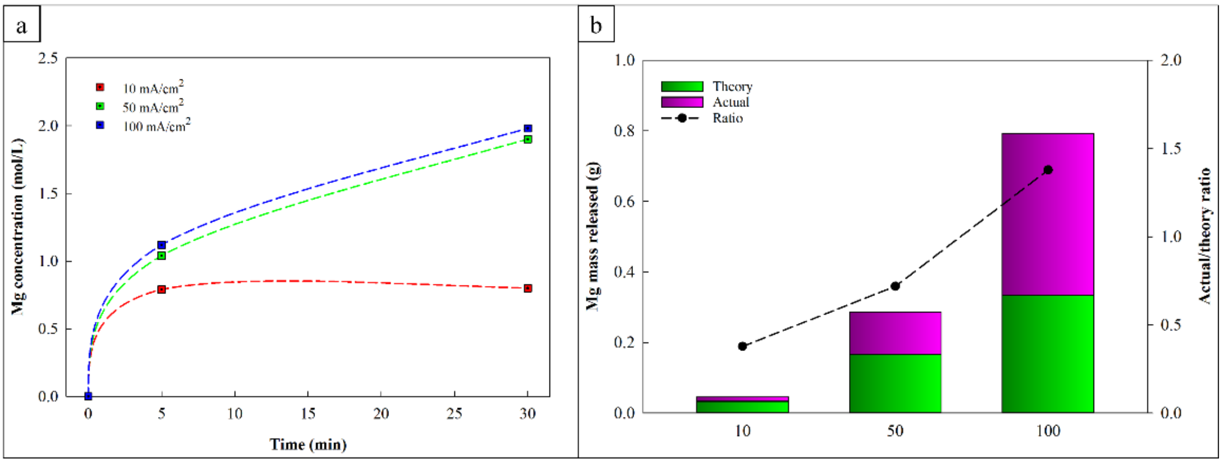

Figure 2. The effect of current density on the (a) releasing Mg ions; (b) actual/theoretical ratio

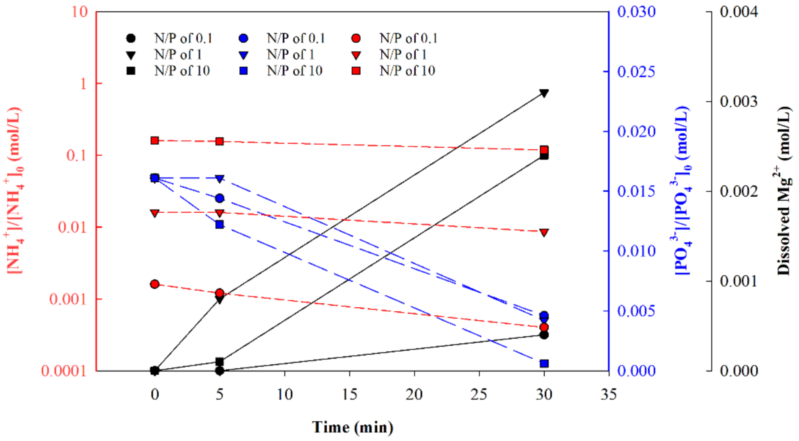

Figure 3. Dissolved Mg ions, ammonium reduction, and phosphate reduction under different N/P molar ratios

For both ammonium and phosphate, an increase in the concentration in the test solution decreased the reduction ratio. At an N/P variation of 1:10, ammonium was reduced by 77.19%. In the N/P of 1:1 and 10:1 variation, ammonium was reduced by 46.91% and 26.28%, respectively. On the other hand, in the N/P variation of 10:1, where the phosphate concentration was the lowest among the other variations, phosphate also experienced the highest reduction, reaching 96.38%. At N/P ratios of 1:1 and 1:10, phosphate reduction decreased to 74.26% and 71.41%, respectively. This shows that the higher the content of ammonium and phosphate in the test solution, the reduction was due to an increase in the pollutant load while other pollutants (Mg^{2+} ions) reached their limits.

3.3. Mass precipitates

After 30 minutes of experiments, the precipitate formed was collected and weighed as a wet mass. Figure 4 shows that the N/P molar ratio of 10:1 produced the highest mass of precipitate, approximately 4.1914 grams, followed by the 1:10 ratio approximately 3.4379 grams. The 1:1 N/P molar ratio resulted in the lowest precipitate mass (approximately 3.1139 g). This indicates that a higher nitrogen concentration leads to a greater amount of precipitate formation during electrolysis.

The increase in precipitate mass at the 10:1 N/P molar ratio was due to the higher availability of ammonium ions in the solution, which enhanced the potential for struvite crystallization. This is in accordance with previous studies reporting that higher concentrations of ammonium ions lead to increased precipitation of struvite (Wang et al., 2022). The sacrificial magnesium anode provided the essential magnesium ions needed for struvite formation. These ions consisted of magnesium, ammonium, and phosphate.

3.4. Precipitate morphological analysis

The precipitate crystals observed under a microscope exhibit various shapes and sizes, reflecting the conditions under which they were formed. In the first image (Figure 5a), the crystals are predominantly elongated and needle-like, with some exhibiting a prismatic form. The crystals were well-defined and their length varied, indicating a range of growth stages. The clarity and sharp edges suggest that the formation conditions were relatively stable, allowing for the gradual growth of the structures. In the second image (Figure 5b), the crystals appear to be more fragmented, with irregular shapes and a higher degree of clustering. This may indicate either a disturbance in the growth environment or the initial stages of crystal aggregation. The fragments could be caused by mechanical stress or fluctuations in the conditions, such as pH or temperature,

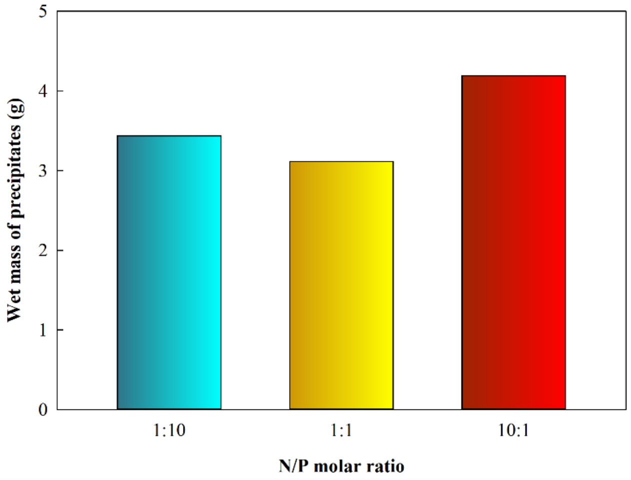

Figure 4. Wet mass of precipitates under different N/P molar ratio

during the crystallization process. The third image (Figure 5c) shows a mix of larger, more defined crystals and smaller, less distinct fragments. The presence of both well-formed and fragmented crystals could indicate variations in the local environment, such as changes in supersaturation levels or the presence of impurities that may have affected crystal growth.

Based on SEM analysis, it was established that the precipitate of the third variation of the N/P molar ratio had a morphology similar to that of the precipitate of struvite in general. With increasing ammonium concentration, the precipitate of struvite appears to have a larger volume and a smoother surface. As the quantity of ammonium increased, the angle of the formed crystals became increasingly dull, and the morphology of the precipitate became more pronounced (Li et al., 2024). Based on the EDS analysis, the three variations exhibited peaks for the elements Mg, O, and P, which are the forming elements of struvite. At the 1:10 and 1:1 variation, the spectrum intensities of Mg, O, and P were higher than those at the 10:1 variation (Figure 6).

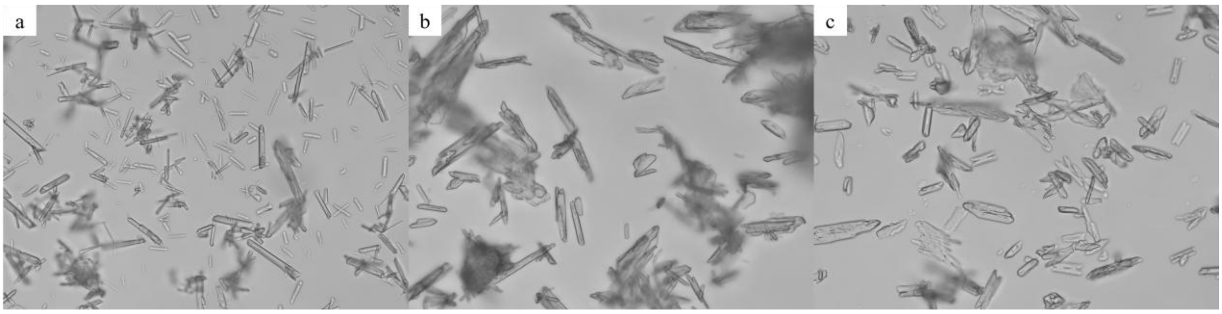

Figure 5. Visualization of precipitates formed at different N/P molar ratios

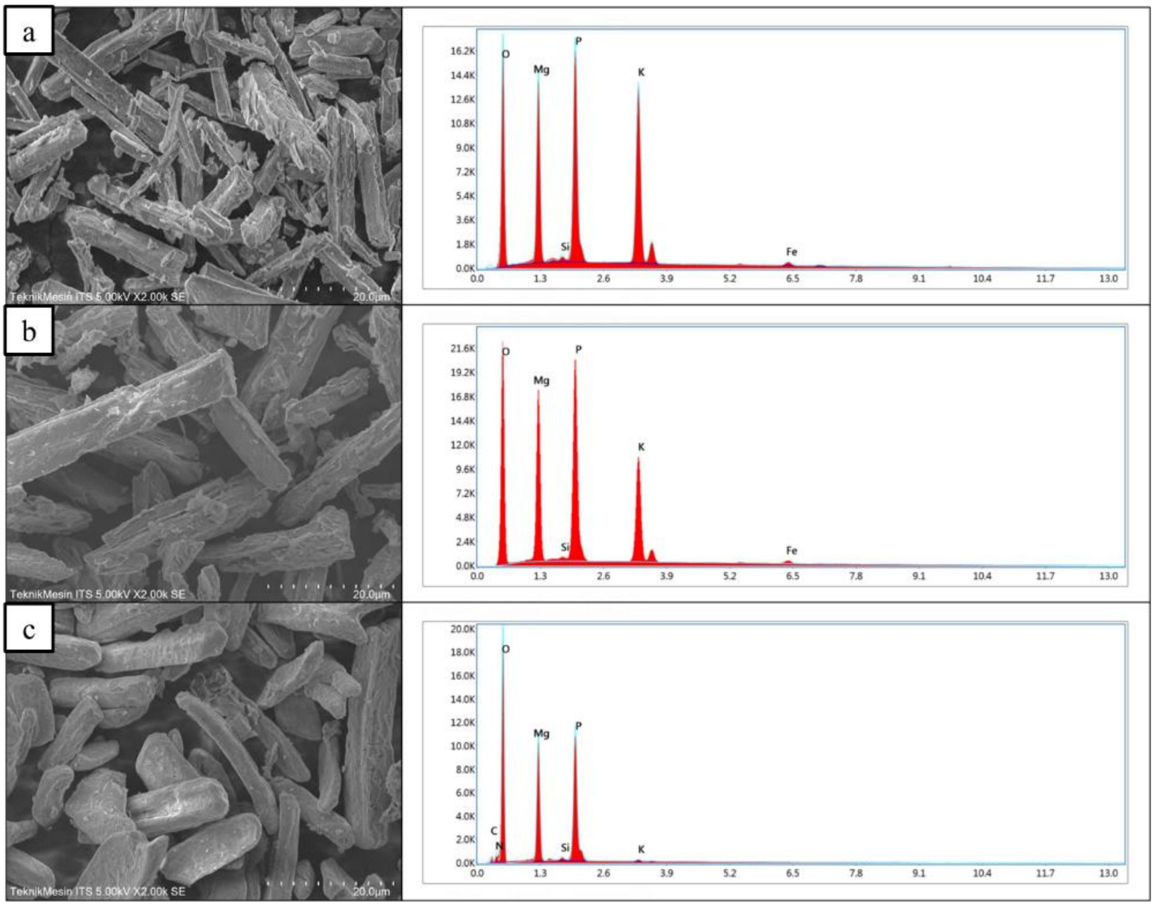

Figure 6. Precipitates morphology by SEM-EDS at N/P of (a) 1:10; (b) 1:1; (c) 10:1

The EDS data were then input into Visual MINTEQ 3.1 software to model the possible precipitation. Of the three N/P molar ratio variations, only the 10:1 N/P molar ratio variation was identified as struvite and magnesium phosphate precipitates with saturation index of 1.557 and 0.641, respectively. The remaining two variations identified only magnesium phosphate precipitate with a saturation index of 1.332 for an N/P molar ratio variation of 1:10 and 1.497 for an N/P molar ratio variation of 1:1. This indicated that at the 1:10 and 1:1 molar ratio, the formation of magnesium phosphate was more dominant than the formation of struvite because the ammonium concentration was not high enough to form struvite.

3.5. Energy consumption

The N/P molar ratio of 1:10 exhibited the highest energy consumption per mg phosphate (approximately 0.090 Wh), followed by the N/P molar ratio of 1:1 (approximately 0.055 Wh), and the N/P molar ratio of 10:1 had the lowest (0.011 Wh) (Figure 7). The reduction in energy consumption at an N/P molar ratio of 10:1 suggested that this ratio enabled more efficient struvite formation, possibly due to nitrogen-rich conditions facilitating ion transfer during the electrolysis process. The energy consumption for all these variations (with an electrode gap of 2 cm) was much lower than those of the Hug and Udert (2013) and Zheng et al (2009) studies, which were 2.2 Wh/mg-P with an electrode gap of 5.5 cm and 8 Wh/mg-P with an electrode gap of 5 cm, respectively. These results support Zheng et al. (2009) report that the electrode gap can reduce energy consumption.

Different molar ratios appeared to alter the electrochemical environment around the magnesium anode, which subsequently influenced the energy consumption. A higher N/P ratio (10:1) reduces the resistance within the solution, allowing reactions to occur with lower energy input. This finding is significant for optimizing processes in terms of energy efficiency and cost-effectiveness, particularly in applications aimed at sustainability on a larger scale.

4. Conclusion

In conclusion, the dissolution of Mg ions from magnesium plates during electrolysis is influenced by the current density. As the current density increased, the dissolution rate of Mg ions also increased; however, it was essential to consider the actual-to-theoretical ratio to achieve energy efficiency targets. Based on the conducted experiments, an optimum current density of 50 mA/cm^2 was determined.

Additionally, the formation of struvite through electrolysis with a magnesium anode depended on the N/P molar ratio of the test solution, which was consistent with the known factors affecting struvite crystallization. The ammonium and phosphate reduction ratios at a 1:1 molar

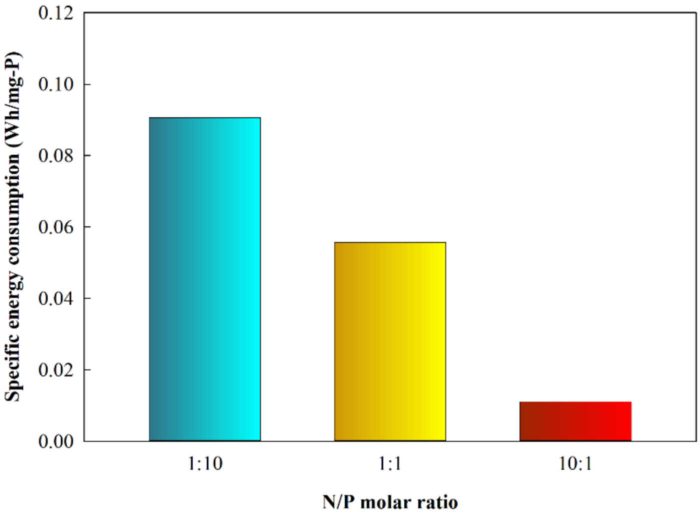

Figure 7. The energy consumption of the electrolysis under different N/P molar ratio

ratio was approximately 46.91% and 74.26%, respectively. Increasing the ammonium molarity in the test solution to 10:1 increased the phosphate reduction ratio to 96.38% while decreasing the ammonium reduction ratio to 26.28%. The maximum precipitation of 4.1914 g was generated at a molar ratio of 10:1 with a specific energy consumption of 0.011 Wh/mg-P, out of the three ammonium/phosphate molar ratio variations.

Acknowledgment

The authors would like to acknowledge the Ministry of Education, Culture, Research, and Technology of the Republic of Indonesia for the financial support (038/E5/PG.02.00.PL/2024 and 1740/PKS/ITS/2024) under the Fundamental Research Scheme.

References

Bagastyo, A. Y., Anggrainy, A. D., Khoiruddin, K., Ursada, R., Warmadewanthi, I. D. A. A., & Wenten, I. G. (2022). Electrochemically-driven struvite recovery: Prospect and challenges for the application of magnesium sacrificial anode. Separation and Purification Technology, *288*, 120653. https://doi.org/10.1016/j.seppur.2022.120653

Cai, Y., Han, Z., Lin, X., Du, J., Lei, Z., Ye, Z., & Zhu, J. (2022). Mechanisms of releasing magnesium ions from a magnesium anode in an electrolysis reactor with struvite precipitation. Journal of Environmental Chemical Engineering, *10*(1), 106661. https://doi.org/10.1016/j.jece.2021.106661

Hug, A., & Udert, K. M. (2013). Struvite precipitation from urine with electrochemical magnesium dosage. Water Research, *47*(1), 289–299. https:/doi.org/10.1016/j.watres.2012.09.036

Kékedy-Nagy, L., Teymouri, A., Herring, A. M., & Greenlee, L. F. (2020). Electrochemical removal and recovery of phosphorus as struvite in an acidic environment using pure magnesium vs. the AZ31 magnesium alloy as the anode. Chemical Engineering Journal, *380*, 1–7. https://doi.org/10.1016/j.cej.2019.122480

Kim, D., Ryu, H. D., Kim, M. S., Kim, J., & Lee, S. I. (2007). Enhancing struvite precipitation potential for ammonia nitrogen removal in municipal landfill leachate. Journal of Hazardous Materials, *146*(1–2), 81–85. https://doi.org/10.1016/j.jhazmat.2006.11.054

Li, L., Bi, J., Sun, M., Wang, S., Guo, X., Li, F., Liu, J., & Zhao, Y. (2024). The Simultaneous Efficient Recovery of Ammonia Nitrogen and Phosphate Resources in the Form of Struvite: Optimization and Potential Applications for the Electrochemical Reduction of NO3−. Molecules, *29*(10), 2185. https://doi.org/10.3390/molecules29102185

Lin, J. L., & Sidik, F. (2024). Harvesting of cyanobacteria and phosphorus by electrocoagulation-flocculation-flotation: Role of phosphorus precipitation in cell separations and organics destabilization. Water Research, *259*, 121868. https://doi.org/10.1016/j.watres.2024.121868

Lin, J. L., Sidik, F., & Kang, S. F. (2023). Harvesting of microcells from cyanobacteria-laden water by energy-efficient electro-flocculation-flotation with aluminum hydrates. Journal of Water Process Engineering, *52*, 103585. https://doi.org/10.1016/j.jwpe.2023.103585

Luo, W., Fang, Y., Song, L., & Niu, Q. (2022). Production of struvite by magnesium anode constant voltage electrolytic crystallisation from anaerobically digested chicken manure slurry. Environmental Research, *214*(4), 113991. https://doi.org/10.1016/j.envres.2022.113991

Natsi, P. D., & Koutsoukos, P. G. (2024). Electrochemical Recovery of N and P from Municipal Wastewater. Crystals, *14*(8), 675. https://doi.org/10.3390/cryst14080675

Siciliano, A., Limonti, C., Curcio, G. M., & Molinari, R. (2020). Advances in struvite precipitation technologies for nutrients removal and recovery from aqueous waste and wastewater. Sustainability (Switzerland), *12*(18), 7538. https://doi.org/10.3390/su12187538

Silva-Gálvez, A. L., López-Sánchez, A., Camargo-Valero, M. A., Prosenc, F., González-López, M. E., & Gradilla-Hernández, M. S. (2024). Strategies for livestock wastewater treatment and optimised nutrient recovery using microalgal-based technologies. *Journal of Environmental Management*, *354*, 120258. https://doi.org/10.1016/j.jenvman.2024.120258

Vaishnav, S., Saini, T., Chauhan, A., Gaur, G. K., Tiwari, R., Dutt, T., & Tarafdar, A. (2023). Livestock and poultry farm wastewater treatment and its valorization for generating value-added products: Recent updates and way forward. *Bioresource Technology*, *382*, 129170. https://doi.org/10.1016/j.biortech.2023.129170

Wang, L., Gu, K., Zhang, Y., Sun, J., Gu, Z., Zhao, B., & Hu, C. (2022). Enhanced struvite generation and separation by magnesium anode electrolysis coupled with cathode electrodeposition. *Science of the Total Environment*, *804*, 150101. https://doi.org/10.1016/j.scitotenv.2021.150101

Ye, Y., Ngo, H. H., Guo, W., Liu, Y., Chang, S. W., Nguyen, D. D., Liang, H., & Wang, J. (2018). A critical review on ammonium recovery from wastewater for sustainable wastewater management. *Bioresource Technology*, *268*, 749–758. https://doi.org/10.1016/j.biortech.2018.07.111

Zheng, X. Y., Kong, H. N., Wu, D. Y., Wang, C., Li, Y., & Ye, H. R. (2009). Phosphate removal from source separated urine by electrocoagulation using iron plate electrodes. *Water Science and Technology*, *60*(11), 2929–2938. https://doi.org/10.2166/wst.2009.309